ELSEVIER

www.elsevier.nl/locate/jorganchem

Journal of Organometallic Chemistry 607 (2000) 164–174

Journal of Organometallic Chemistry

Theoretical investigation of the formation of five-membered metallacycles by reaction of CO with metallacyclobutenones: differences between Ni and Pt

Stuart A. Macgregor [a,*], Eric Wenger [b]

[a] *Department of Chemistry, Heriot-Watt University, Riccarton, Edinburgh EH14 4AS, UK*
[b] *Research School of Chemistry, Australian National University, Canberra, ACT 0200, Australia*

Received 3 March 2000; accepted 16 May 2000

This paper is dedicated to Professor Martin A. Bennett, a pioneer of organometallic chemistry, on the occasion of his 65th birthday and his retirement from the Australian National University.

Abstract

Reactions of CO with nickel or platinum complexes of cyclic alkynes or arynes form initially metallacyclobutenone species, which undergo further insertion of CO to give five-membered metallacycles. The differences in regioselectivity observed for nickel or platinum have been investigated computationally by DFT methods. Although both metals prefer insertion of the second CO via a five-coordinate mechanism, the formation of the five-membered nickelacycle is under thermodynamic control, leading to a symmetrical nickelacyclopentene-2,4-dione complex, whereas platinum yields the kinetically favoured platinacyclopentene-2,3-dione complex.

Keywords: Platinum; Nickel; Acyl-complex; CO insertion; DFT calculation; Metallacycle

1. Introduction

The insertion of carbon monoxide into a metal–carbon bond is one of the most important reactions in organometallic chemistry [1–3]. Insertion reactions of carbon monoxide or isoelectronic isocyanides into one M–C bond of a metallacycle lead generally to an expansion of the ring [4,5]. However, such metallacycles formed with Group 10 elements are not often observed [6–9]. Subsequent reactions, usually a very fast reductive elimination, give rise to carbo- or heterocyclic organic products. In the case of nickel(0) complexes of benzyne and 4,5-difluorobenzyne, [Ni(dcpe)-(1,2η-4,5-$X_2C_6H_2$)] [X = H (**1**), F (**2**)], insertion of two equivalents of CO occurs [10]. As shown in Scheme 1, the first step is believed to be insertion of one CO, giving a highly reactive and so far unobserved benzonickelacyclobutenone (**3**). A second molecule of CO then inserts into the nickel–aryl bond of **3** to give a phthaloylnickel(II) complex **4**, which, for X = F, has been detected by ^{31}P- and ^{19}F-NMR spectroscopy. An analogous complex can be formed by reaction of [Ni$(CO)_2$(bipy)] with phenylacetylene or [Ni(bipy)(η^2-PhC_2Ph)] with CO [11,12]. Subsequent reactions of complex **4** lead to the benzocyclobutene-1,2-dione (**5**) by reversible elimination of [Ni$(CO)_2$(dcpe)] or the phthalatonickel(II) complex **6** by oxidation with air.

Support for the proposed benzonickelacyclobutenone (**3**) as an intermediate in Scheme 1 is provided by the isolation of analogous complexes containing four-membered rings from the reaction of diphenylcyclopropenone with platinum(0) precursors [13], or by reaction of *t*-butyl isocyanide with [Pt$(PPh_3)_2$(η^2-C_6H_8)] (**7**) (Scheme 2) [14].

In the latter case, further insertion of *t*-BuNC can occur. However, the regioselectivity of this reaction differs from that of the insertion of a second CO molecule in the Ni–C_6H_4 system described above, in that an unsymmetrical platinacycle, **8**, is formed [15].

* Corresponding author.

0022-328X/00/$ - see front matter
PII: S0022-328X(00)00333-8

This difference in regioselectivity was thought to be thermodynamic in origin, as a closely related difference is evident in the reactions of benzocyclobutene-1,2-dione with the nickel(0) complex $[Ni(CO)_2(bipy)]$ and

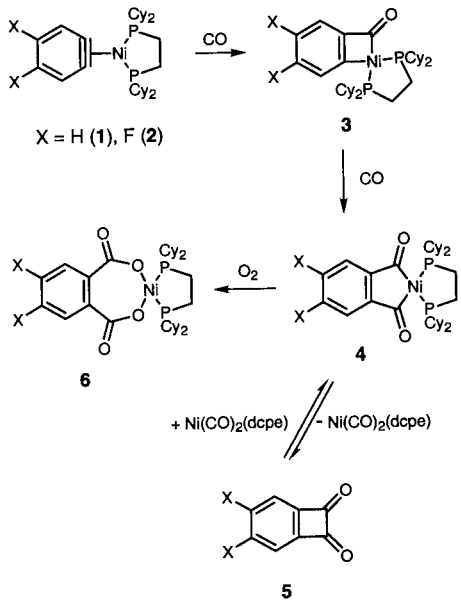

Scheme 1.

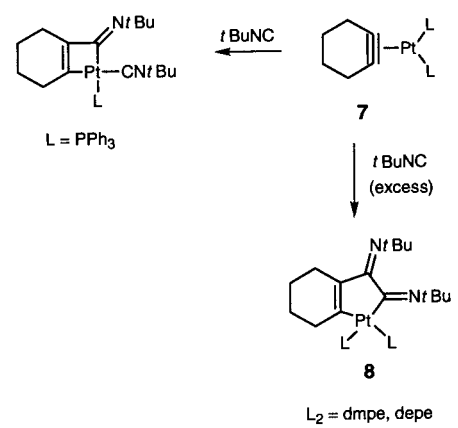

Scheme 2.

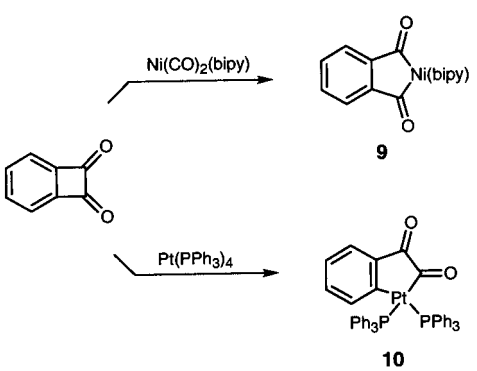

Scheme 3.

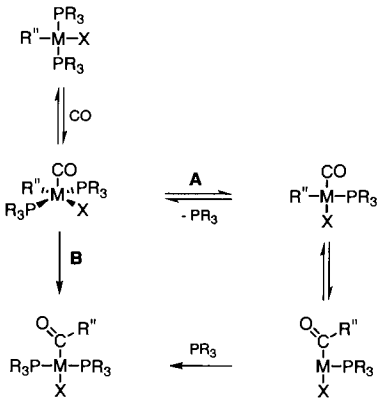

Scheme 4.

with the platinum(0) complex $[Pt(PPh_3)_4]$ (Scheme 3). In the first case, the CO–CO bond is cleaved, giving the phthaloylnickel(II) complex **9** [11,16], whereas in the second case a phenyl–CO bond is cleaved giving the α-ketoacyl complex **10** [17–19].

In this paper we present the results of a density functional computational study undertaken to understand the origin of the different regioselectivities observed for the nickel and platinum systems described above. Our calculations will be based upon the reactions of CO with the model metallacyclobutenone complexes $[M\{CH{=}CHC(O)\}(PH_3)_2]$ (M = Ni, Pt). The computational results indicate that the observed regioselectivities for the CO insertion reactions do not in fact have a simple thermodynamic explanation, but must result from differences in the reaction pathways. We have therefore extended our study to model the mechanism of the CO insertion process and give here a brief overview of the known results in this area.

The mechanisms for the insertion of CO into a Pt–C or Pd–C bond are well documented, but less is known for the corresponding reactions with nickel [20,21]. In the case of the *trans*-complexes $[MX(L)_2(R'')]$ of all Group 10 elements, carbon monoxide has been shown to enter the coordination sphere of the metal in an associative process. However, the insertion into the metal–carbon bond can take place from either a four-coordinated species, where the CO has replaced one of the ligands L (route A, Scheme 4), or from a five-coordinated species (route B); both mechanisms have been observed for all three metals. Kinetic studies on the *trans*-bisphosphine complexes $[MX(R'')(PR_3)_2]$ (M = Ni, Pd, Pt) have shown that both mechanisms occur simultaneously (Scheme 4) [22].

With excess phosphine, route B is preferred for all metals, but the rate of insertion is fastest for nickel. Under standard conditions, however, insertion into a Ni–C bond is slower than into a Pd–C bond, suggesting that the platinum and palladium complexes favour the dissociative pathway A. The latter pathway also in-

volves isomerisation as, for the platinum complexes, only the isomer with the halide *trans* to CO has been shown to undergo insertion. The reasons for such a preference have been investigated theoretically [23]. In addition, the insertion reaction is very sensitive to the electron-density on the metal. For platinum complexes with less basic phosphines (e.g. R = Ph) pathway A is favoured, but the insertion seems to occur directly from the five-coordinated species with more basic phosphines [24]. In summary, with *trans*-complexes, a dissociative pathway (A) is generally preferred for palladium and platinum, whereas the insertion into a Ni–C bond is more likely to involve a five-coordinate species. CO-bearing five-coordinate Ni systems have been calculated to be stabilised by combinations of phosphine and π-donor ligands [25]. The related $[Pd(CH_3)(NH_3)_3]^+$ system has also been studied both experimentally and theoretically. When this complex is reacted with CO, a five-coordinate species is formed as a transition state, followed by dissociation of one amine ligand with insertion of the CO taking place from a four-coordinate species [26].

Complexes with a *cis*-geometry, especially with chelating ligands, would be more relevant to the metallacycles discussed in this paper, but unfortunately fewer data are available regarding the mechanism of their reactions with CO. As expected for complexes having bidentate ligands, the rigidity of the system favours an associative pathway as the exchange of one ligand for a CO becomes hindered, if not completely stopped [20]. For example, the reactions of the metallacyclopentane complex $[\overline{Ni(CH_2CH_2CH_2CH_2)}L_2]$ with CO are fast when $L = PPh_3$, but no insertion occurs when L_2 = dppe, as this complex is reluctant to form a five-coordinate species [27]. Also, the complex *cis*-$[PtPh_2L_2]$ inserts CO when L is a monodentate tertiaryphosphine, but no insertion is observed when L_2 is a chelating ligand; the reaction has been shown to follow a dissociative pathway [28]. A study of $[Pd(PP)(Me)(L)]^+$ (PP = dppe, dppp) has shown that the rate of the CO insertion follows the ease of replacement of L by CO, indicating that CO requires a coordination site on a square planar palladium centre [29].

Many studies with bidentate P–N and N–O ligands have been reported recently [21,30–33]. In platinum complexes, the nitrogen end of the bidentate ligand has to dissociate to give way to CO for the insertion to occur. Similar studies using pyridine carboxylate (pyca) ligands have shown that carbonylation of the platinum complexes $[PtR(PPh_3)(pyca)]$ proceeds via a square-planar intermediate where CO has replaced the phosphine ligand or sometimes the N-end of pyca (dissociative pathway) [34]. For the nickel analogues, the mechanism is not so clear. Ethene oligomerisations catalysed by these complexes are insensitive to excess phosphine, suggesting a five-coordinate associative pathway, but CO–ethene copolymerisation seems to prefer the dissociative route [35,36].

Overall, the examples described above seem to indicate that insertion of CO into Ni–C bonds is more likely to occur from a five-coordinate intermediate, whereas carbonylation of analogous platinum complexes tends to take place from a four-coordinate species arising from replacement of one auxiliary ligand by CO.

2. Computational details

All calculations used the Amsterdam Density Functional program (ADF, version 2.3.1) developed by Baerends et al. [37,38], and employed the numerical integration scheme of te Velde and Baerends [38]. A triple-ζ-STO basis set was employed for the metal atoms while all other atoms were described using a double-ζ-STO basis set extended by a polarisation function. An auxiliary set of s, p, d, f and g STO basis functions centred on all nuclei was used in order to fit the molecular density and describe accurately the coulomb and exchange potentials in each SCF cycle [39]. Core electrons (the 1s electrons for C and O and up to and including 2p for P and Ni and 4f for Pt) were treated using the frozen core approximation. Geometry optimisation was carried out using the local density approximation employing the parameterisation of Vosko et al. [40] and used the optimisation procedure developed by Versluis and Ziegler [41]. The quasi-relativistic corrections of Ziegler and co-workers were also included [42]. Energies of all optimised structures were then recalculated with the non-local corrections of Becke [43] (exchange) and Perdew [44] (correlation) included. The geometries of all three- and four-coordinate species were fully optimised in either C_s or, where appropriate, C_{2v} symmetry. For five-coordinate species lower symmetry structures were located. Frequency analyses, run with the internal motions of the PH_3 ligands frozen in order to reduce the computation time, confirmed the stationary points obtained were true minima. Reaction profiles for CO insertion from four-coordinate reactant molecules were computed in C_s symmetry while no symmetry constraints were imposed on reaction profiles originating from five-coordinate species. Once located, the nature of the transition state structures were assessed by a frequency calculation. During our study it became clear that, in particular for the five-coordinate species, several different apparent insertion products lie on the potential energy surface. Time and computing requirements precluded a full tracing of the intrinsic reaction coordinate from each transition state structure, however approximate reaction pathways were attempted by adding 10% of the unique imaginary frequency onto the transition state

structure and allowing the system to relax to the product geometry. With the exception of those cases mentioned in the text the expected planar five-membered metallacycle geometry was always obtained from this approach.

3. Results and discussion

3.1. Reactants, products and overall energetics of CO insertion

Optimized geometries and relative energies for the [M{CH=CHC(O)}$(PH_3)_2$] reactant complexes [**11**, M = Ni; **12**, M = Pt], the symmetrical metallacyclopentenedione product complexes [**13**, M = Ni; **15**, M = Pt] and unsymmetrical α-ketoacyl product complexes [**14**, M = Ni; **16**, M = Pt] are shown in Fig. 1. All structures show the expected distorted square-planar geometries with, in the unsymmetrical species, M-P bonds trans to the acyl groups being slightly longer. In all cases, the five-membered metallacycles are computed to be more stable than the reactants, indicating that CO insertion to both products is exothermic. In addition, the symmetrical metallacyclopentenedione complexes of both metals are calculated to be more stable than the corresponding α-ketoacyl species (by 44.3 and 46.4 kJ mol^{-1} for M = Ni and Pt, respectively). These results rule out a simple thermodynamic explanation for the experimental data and suggest that the observed regioselectivities can only arise from differences in the reaction pathways. We have therefore extended our work to include a study of the mechanism of CO insertion with metallacyclobutenones.

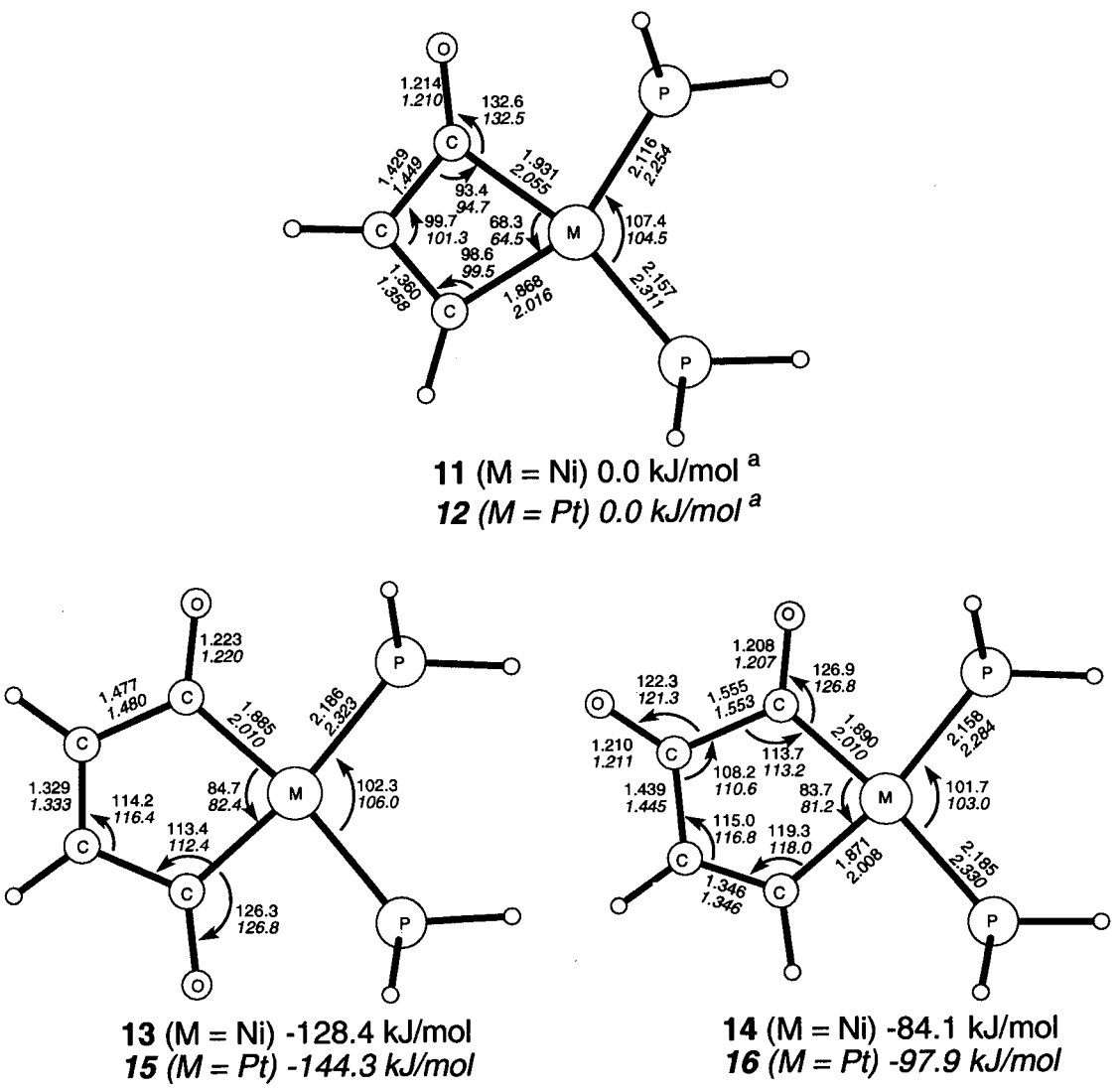

Fig. 1. Optimised geometries (Å, °) and relative energies for metallacyclobutenone reactant and metallacyclopentenedione and α-ketoacyl product complexes. (a) These relative energies incorporate the computed energy of free CO.

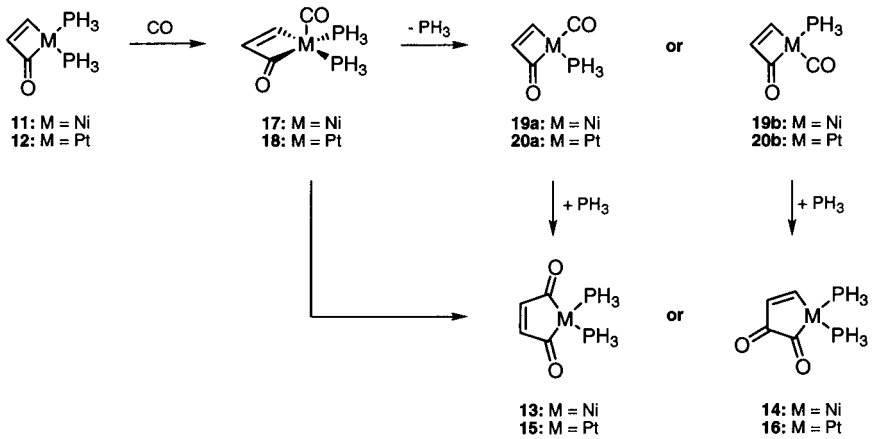

Scheme 5.

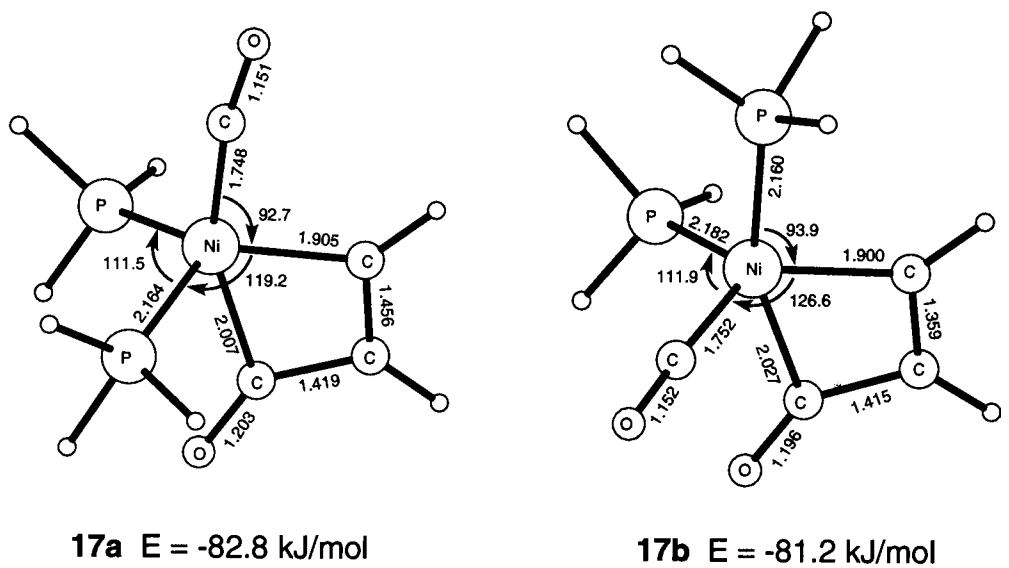

Fig. 2. Optimised geometries (Å, °) and relative energies of five-coordinate nickel intermediates.

3.2. Reaction pathways

The basis of our model calculations is shown in Scheme 5. We have considered direct insertion from five-coordinate intermediates (**17**, M = Ni; **18**, M = Pt) and the alternative pathway involving PH_3 dissociation and subsequent CO insertion from four-coordinate species (**19a**/**b**, M = Ni; **20a**/**b**, M = Pt).

3.2.1. Reaction intermediates

Several isomeric forms for the five-coordinate intermediates **17** and **18** may exist and initial calculations assessed all possible trigonal bipyramidal geometries. Geometries were fully optimised, initially in C_s symmetry if appropriate, with subsequent calculations run without any symmetry constraints. For nickel, this approach located two low energy minima, both of which have a distorted trigonal bipyramidal geometry (Fig. 2). Isomer **17a** exhibits C_s symmetry with the CO ligand in an axial position, *cis* to the Ni–C(H) bond, while in **17b** (C_1 symmetry) CO occupies an equatorial site *cis* to the axial Ni–C(O) bond. The relative energies of these species are very similar and indicate CO ligand binding energies of around 80 kJ mol^{-1}. A third trigonal bipyramidal structure, with C_s symmetry, was found in which the CO ligand occupies an axial position *cis* to Ni–C(O). This species is about 17 kJ mol^{-1} higher in energy than **17b** and may be involved in intramolecular phosphine exchange processes in that species, although this point was not investigated any further at the present time.

The two lowest energy five-coordinate species optimised for the platinum system are shown in Fig. 3. In contrast to the nickel case, the structures here are better described as distorted square-pyramidal with a PH_3 ligand occupying the axial site and CO *cis* to either the Pt–C(H) bond (**18a**) or the Pt–C(O) bond (**18b**). Compared with the Ni system, the computed CO binding

energies are much lower, being approximately 18 kJ mol^{-1}. Two additional trigonal bipyramidal structures were also located, both exhibiting C_s symmetry with the CO ligand in an axial position either *cis* to Pt–C(H) or Pt–C(O). These structure were computed to lie only 8–12 kJ mol^{-1} higher in energy than **18a**/**b** and again may be involved in phosphine exchange pathways.

Structures and relative energies for the two isomeric forms of the four-coordinate species formed via PH_3 loss from **17** and **18** are shown in Fig. 4 (**19a**/**b**, M = Ni; **20a**/**b**, M = Pt). For each metal, the two isomers are very similar in energy. However, for nickel the four-coordinate are about 40 kJ mol^{-1} less stable relative to the five-coordinate species **17a**/**b**, whereas for platinum the four- and five-coordinate complexes are of comparable energy.

3.2.2. Reaction pathways: dissociative

The transition states for CO insertion from four-coordinate **19b** and **20a**/**b** as well as the resultant three-coordinate metallacycle product species (**21a**/**b**, M = Ni; **22a**/**b**, M = Pt) are shown in Fig. 4. Transition states were initially located in C_s symmetry and, with the exception of insertion into the Ni–C(H) bond (see below), were characterised as having one imaginary frequency. The reaction to give the three-coordinate products is more favourable for insertion into M–C(H) bonds, this being exothermic by 13–28 kJ mol^{-1} compared to the slightly endothemic insertion into M–C(O) bonds. Geometries within the metallacycle products are similar to those of **13**–**16**, with the exception of shorter M–C bonds *trans* to the vacant site. The most stable form of the α-ketoacyl products has the vacant site *trans* to the acyl group.

For the CO insertion reaction of **19a** a transition state structure with a computed relative energy of + 123.8 kJ mol^{-1} was located in C_s symmetry. However, this species exhibited two imaginary frequencies, one of which broke the plane of symmetry. In addition, as the reaction profile proceeded the P–Ni–$C_{carbonyl}$ angle stayed roughly constant and the in-plane imaginary frequency was found to correspond to a degenerate CO insertion/deinsertion process leading back to **19a** rather than the expected three-coordinate product **21a**. Attempts to avoid this by constraining the P–Ni–$C_{carbonyl}$ angle to 90° led to a C_s 'transition state' structure about 12 kJ mol^{-1} higher in energy which, still within the C_s symmetry constraint, collapsed to the previous second order transition state once the constraint on the P–Ni–$C_{carbonyl}$ angle was removed. No further efforts to locate this CO insertion transition state were made as it became apparent that insertion via a five-coordinate intermediate is favoured greatly (see below).

The calculated energies of the transition states obtained for the four-coordinate dissociative pathway reveal significant barriers to CO insertion. For M = Pt, the barrier for insertion into the M–C(O) bond is lower than that for insertion into the M–C(H) bond. Consistent with this is the earlier transition state geometry (in terms of C–C bond formation) calculated in the pathway leading to the α-ketoacyl species **22b**. Both reactions are calculated to have higher barriers than that calculated for the insertion of CO into the Pt–CH_3 bond in square-planar [$PtH(CH_3)(CO)(PH_3)$] [45]. Insertion into M–C(O) bonds is easier for M = Ni compared to M = Pt by 57 kJ mol^{-1}.

3.2.3. Reaction pathways: associative

An extensive set of calculations exploring the potential energy surface for CO insertion into the Pt–C(O) bond of **18b** was performed and revealed two general pathways by which the reaction may proceed in the

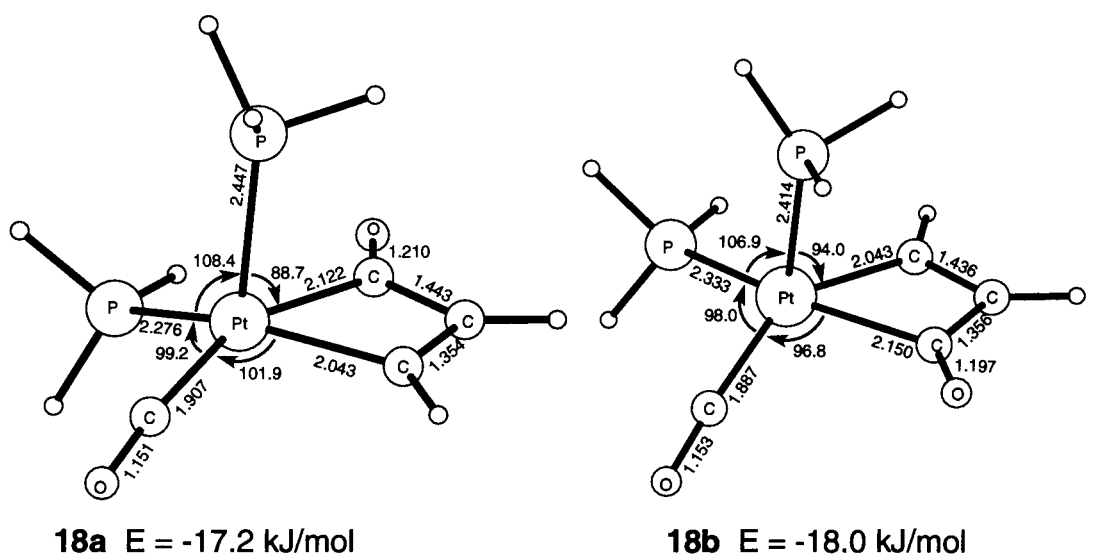

Fig. 3. Optimised geometries (Å, °) and relative energies of five-coordinate platinum intermediates.

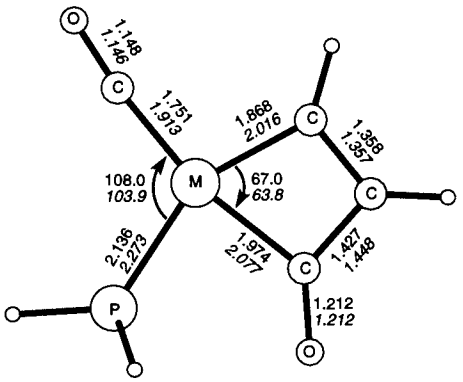

19a (M = Ni) -41.0 kJ/mol
20a *(M = Pt) -18.8 kJ/mol*

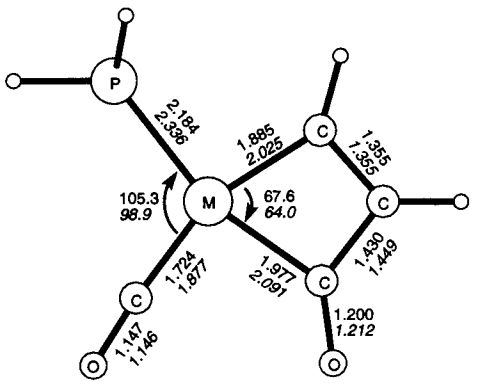

19b (M = Ni) -38.1 kJ/mol
20b *(M = Pt) -23.4 kJ/mol*

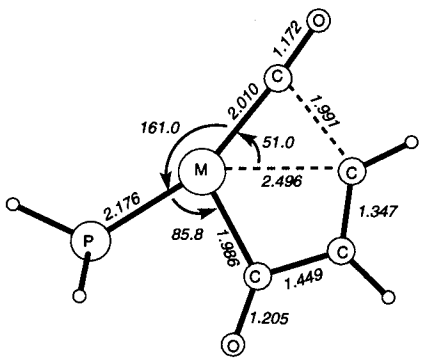

TS ***20a*** $\rightarrow$ ***22a*** *(M = Pt) +216.7 kJ/mol*

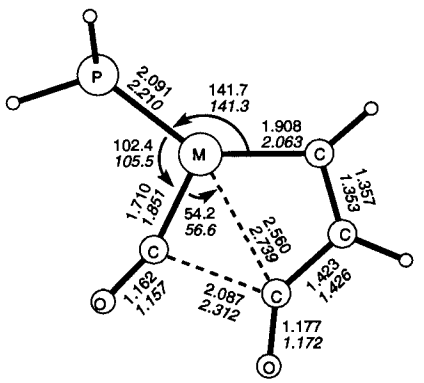

TS 19b $\rightarrow$ **21b** (M = Ni) +93.7 kJ/mol
TS ***20b*** $\rightarrow$ ***22b*** *(M = Pt) +150.2 kJ/mol*

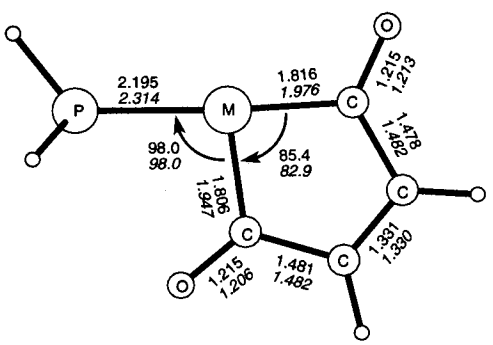

21a (M = Ni) -54.4 kJmol
22a *(M = Pt) -47.3 kJ/mol*

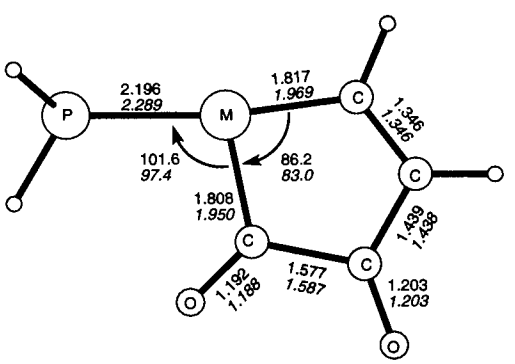

21b (M = Ni) -28.9 kJ/mol
22b *(M = Pt) -23.0 kJ/mol*

Fig. 4. Optimised geometries (Å, °) and relative energies of reaction intermediates, transition states and three-coordinate product complexes for CO insertion via a dissociative mechanism. All energies include the contribution from the free phosphine ligand.

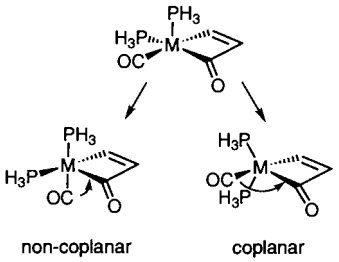

Scheme 6.

five-coordinate systems. From structure **18b** (initially C_1 symmetry) one possibility is for the CO ligand to approach the metallacyclobutenone in an essentially coplanar arrangement. In this case the overall geometry of the molecule near the transition state is close to C_s symmetry. Alternatively, the CO ligand may move further below the metallacyclobutenone plane and approach in a non-coplanar geometry (Scheme 6). Both possibilities were explored for the four CO insertion reactions arising from structures **17** and **18**.

For insertion into the Ni–C(O) bond of **17b** the two alternative transition state structures were found to be very close in energy. The structure shown in Fig. 5 corresponds to the coplanar pathway and is 16.7 kJ mol^{-1} more stable than the isolated reactants. The non-coplanar transition state lies only 1 kJ mol^{-1} higher in energy than this species. Both transition states are therefore approximately 110 kJ mol^{-1} more stable than the transition state located for insertion into the Ni–C(O) bond via a dissociative process.

Tracing the forward pathway from the five-coordinate coplanar transition state led to a new apparent insertion product with approximate C_s symmetry. This species (**23**) has a structure related to a trigonal bipyramid in which one axial ligand is missing and lies less than 4 kJ mol^{-1} higher than the planar α-ketoacyl product. Tracing the reaction forward from the non-coplanar transition state does lead directly to the planar α-ketoacyl product.

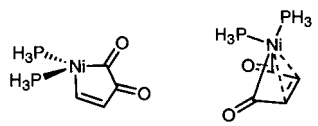

23 **24**

The CO insertion pathway into the Ni–C(H) bond of **17a** shows a preference for the coplanar transition state shown in Fig. 5. This lies 22.6 kJ mol^{-1} higher in energy compared to the isolated reactants and, by analogy with data computed for insertion into Ni–C(O) bonds, is likely to be significantly more stable than the transition state for the dissociative CO insertion mechanism. Following the reaction pathway down from the five-coordinate transition state structure revealed a different type of CO insertion product (**24**) in which the butene-1,4-dione moiety is bound in an η^4-fashion to the metal centre. This species is computed to lie 77.0 kJ mol^{-1} below the isolated reactants and may be an important intermediate in the oxidative addition of cyclobutenones to Group 10 ML_2 fragments. The rearrangement of this species to the final planar metallacyclopentenedione was not studied here, but if we assume the activation barrier associated with this rearrangement will be lower than that of the initial CO insertion step the overall activation energy is over 39 kJ mol^{-1}

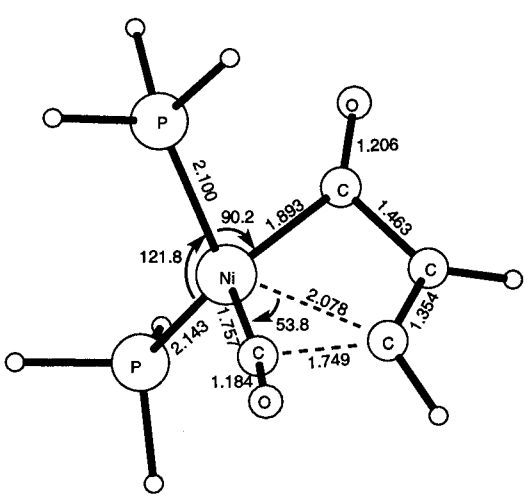

TS 17a → 13 E = +22.6 kJ/mol

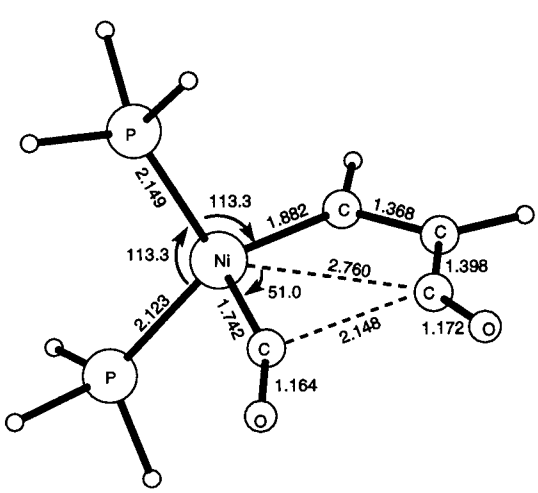

TS 17b → 14 E = -16.7 kJ/mol

Fig. 5. Optimised geometries (Å, °) and relative energies of transition states for CO insertion with nickel via an associative mechanism.

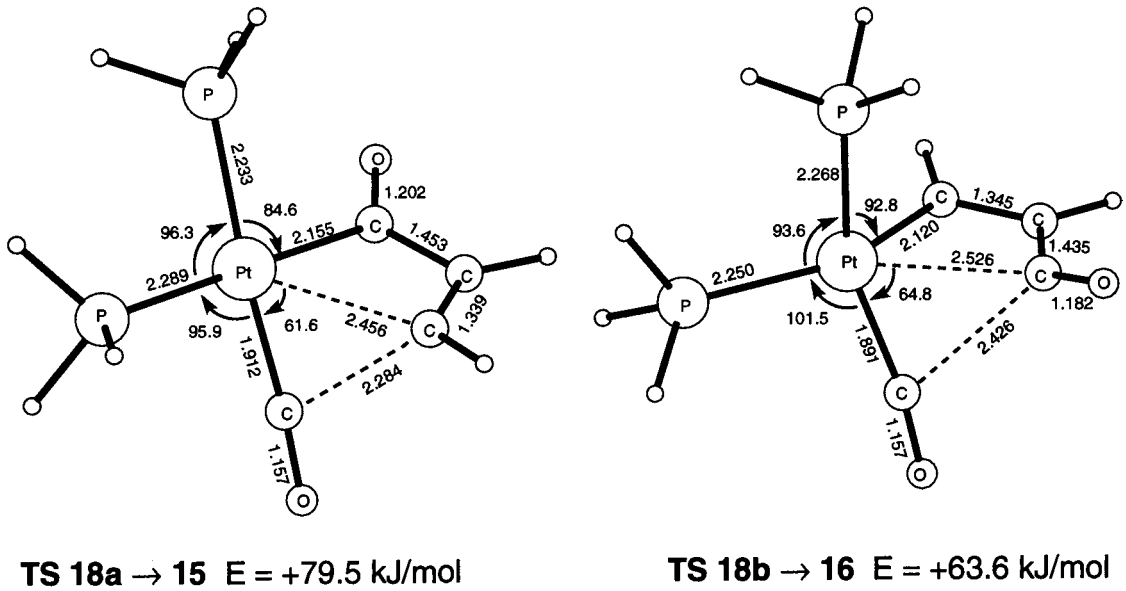

Fig. 6. Optimised geometries (Å, °) and relative energies of transition states for CO insertion with platinum via an associative mechanism.

higher than that associated with CO insertion into the Ni–C(O) bond of **17b**.

In contrast to the nickel case, CO insertion from the platinum intermediates **18a** and **18b** showed a strong preference for a non-planar pathway. The transition states shown in Fig. 6 are estimated to lie approximately 80 kJ mol^{-1} lower than transition states for the coplanar CO insertion pathway. Consistent with previous results, the barrier for insertion into the Pt–C(O) bond is lower (by about 16 kJ mol^{-1}) and the C–C bond forming distance longer (2.43 cf. 2.28 Å) than the corresponding transition state for insertion into the Pt–C(H) bond. Compared to the four-coordinate species, activation energies are lower by 86.6 and 137 kJ mol^{-1} (for insertion into the Pt–C(O) and Pt–C(H) bonds, respectively).

The calculations clearly indicate that for these metallacyclobutenone systems the most accessible transition states for CO insertion are formed via associative mechanisms. For a given mechanism, insertion into a M–C(O) bond entails a lower activation barrier. In addition, barriers for insertion into Pt–C bonds are 60–80 kJ mol^{-1} higher than those for insertion into Ni–C bonds.

4. Discussion

The results of our density functional calculations suggest that formation of the five-membered metallacycles from the model metallacyclobutenone complexes $[\overline{M\{CH{=}CHC(O)\}}(PH_3)_2]$ is most likely to proceed via associative mechanisms and the computed reaction profiles for these processes are summarised in Fig. 7. In the case of nickel, the two possible isomers of **17** are about 80 kJ mol^{-1} more stable than **11** (+ free CO) and 40 kJ mol^{-1} more stable than the equivalent four-coordinate intermediates (+ free PH_3). Subsequent insertion from the five-coordinate intermediates will be faster as a result of lower overall activation energies. In terms of activation barriers insertion into the Ni–CO bond is favoured. However, the difference in energy between the product five-membered nickelacycle **14** and the five-coordinate precursor **17**, is relatively small allowing the reaction to be reversible. Furthermore, the energy of the transition state leading to the more stable symmetrical nickelapentenedione complex **13**, resulting from the insertion of CO into the Ni–C(H) bond, is only 22.6 kJ mol^{-1}, allowing the reaction to be under thermodynamic control.

In the case of platinum, the five-coordinate mechanism is also favoured, but will be much slower than for nickel due to the larger transition state energies. This is in agreement with the kinetic data obtained for $[MX(R'')(PR_3)_2]$ (M = Ni, Pd, Pt) when excess phosphine was added to favour the associative insertion of CO [22]. One explanation for the preference for the unsymmetrical α-ketoacyl product seen experimentally is that this reaction proceeds under kinetic control. The lowest energy transition state (+ 63.6 kJ mol^{-1}) is that for the insertion of CO into the Pt–CO bond of the five-coordinate species **18b**, leading to the α-ketoacyl complex **16**. Under the conditions where these insertions occur (generally room temperature), the barrier will be too high for the reaction to be reversible (about 160 kJ mol^{-1}); hence only the kinetic product **16** is observed.

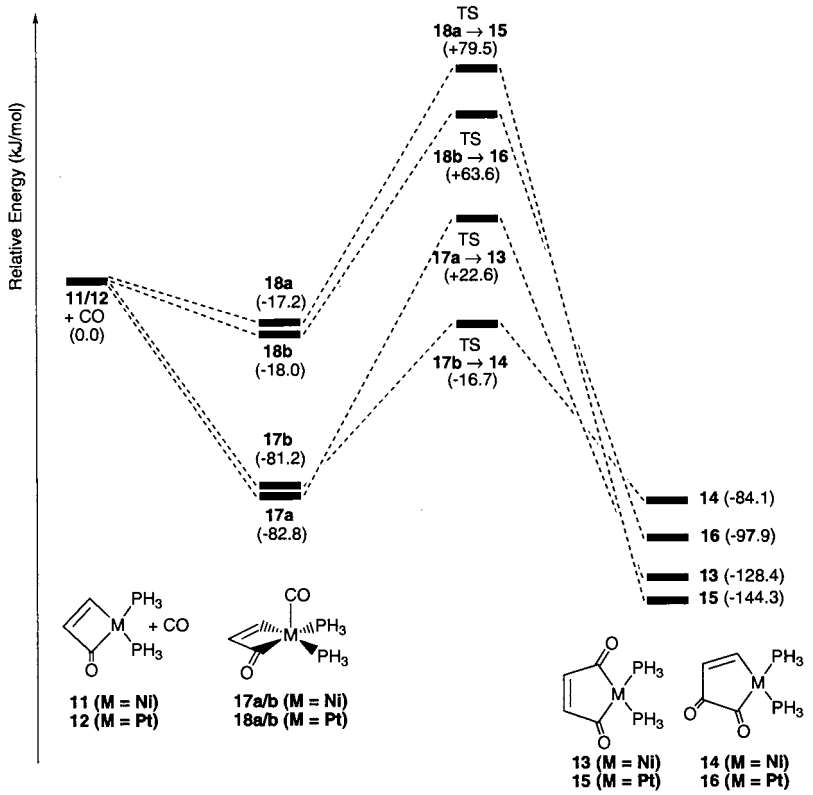

Fig. 7. Reaction profiles for CO insertion via an associative mechanism.

In conclusion, our calculations show that for both M = Ni and Pt the symmetrical metallacyclopentendione complexes are more stable than the isomeric α-ketoacyl species and that, therefore, differences in regioselectivities observed experimentally are not solely thermodynamic in origin. Computed reaction profiles indicate that both metals prefer an associative mechanism for the insertion of CO into either M–C bond of the metallacyclobutenone complex. In addition, computed activation energies are always lower for insertion into a M–C(O) bond compared to a M–C(H) bond. Although the energies required to go from the five-coordinate species **17**/**18** to the corresponding transition states are comparable for both metals, the overall activation energies are much higher for M = Pt due to the high energies of **18a** and **18b**. This is consistent with the general preference for four- over five-coordination in the chemistry of Pt(II) and results in a much more exothermic insertion step with this metal. In contrast five-coordination is more common in the chemistry of Ni(II), and is reflected in the relatively stability of **17a** and **17b** which results in a lower exothermicity for the insertion step with that metal. The difference in regioselectivity observed for the reactions of CO or isocyanides with alkyne or aryne complexes of nickel(0) or platinum(0) can be accounted for by the fact that the second insertion of CO occurs more easily into a Ni–C bond than into a Pt–C bond of the initially formed cyclobutenone or benzocyclobutenone. Hence, the very low energy barrier in the case of nickel allows the formation of the thermodynamically favoured product. In the case of platinum, only the kinetically favoured species will be formed under the experimental conditions.

5. Supplementary material

Optimized Cartesian coordinates of structures **11**–**22** and associated transition states are available from SAM on request.

Acknowledgements

EW gratefully acknowledges the Australian Research Council for the receipt of a QEII Research fellowship. SAM thanks the Royal Society for an equipment grant and the EPSRC for funding.

References

[1] A. Yamamoto, Organotransition Metal Chemistry: Fundamental Concepts and Applications, Wiley, New York, 1986, pp. 251–254.

[2] J.P. Collman, L.S. Hegedus, J.R. Norton, R.G. Finke, Principles and Applications of Organotransition Metal Chemistry, University Science, Mill Valley, CA, 1987.
[3] G.W. Parshall, S.D. Ittel, Homogeneous Catalysis, Wiley, New York, 1992, p. 93.
[4] E. Lindner, Adv. Heterocycl. Chem. 39 (1986) 237.
[5] P.W. Jennings, L.L. Johnson, Chem. Rev. 94 (1994) 2241.
[6] A.K. Smith, in: E.W. Abel, F.G.A. Stone, G. Wilkinson, R.J. Puddephatt (Eds.), Comprehensive Organometallic Chemistry II, vol. 9, Elsevier, Oxford, 1995, p. 29.
[7] A.J. Canty, in: E.W. Abel, F.G.A. Stone, G. Wilkinson, R.J. Puddephatt (Eds.), Comprehensive Organometallic Chemistry II, vol. 9, Elsevier, Oxford, 1995, p. 225.
[8] G.K. Anderson, in: E.W. Abel, F.G.A. Stone, G. Wilkinson, R.J. Puddephatt (Eds.), Comprehensive Organometallic Chemistry II, vol. 9, Elsevier, Oxford, 1995, p. 431.
[9] J. Cámpora, P. Palma, E. Carmona, Coord. Chem. Rev. 193–195 (1999) 207.
[10] M.A. Bennett, D.C.R. Hockless, M.G. Humphrey, M. Schultz, E. Wenger, Organometallics 15 (1996) 928.
[11] H. Hoberg, A. Herrera, Angew. Chem. Int. Ed. Engl. 19 (1980) 927.
[12] A. Herrera, H. Hoberg, R. Mynott, J. Organomet. Chem. 222 (1981) 331.
[13] J. Burgess, R.D.W. Kemmitt, N. Morton, C.T. Mortimer, M.P. Wilkinson, J. Organomet. Chem. 191 (1980) 477.
[14] M.A. Bennett, T. Yoshida, J. Am. Chem. Soc. 100 (1978) 1750.
[15] J.A. Johnson, Ph.D. Thesis, Australian National University, 1991.
[16] H. Hoberg, A. Herrera, Angew. Chem. Int. Ed. Engl. 20 (1981) 876.
[17] J.A. Evans, G.F. Everitt, R.D.W. Kemmitt, D.R. Russell, J. Chem. Soc. Chem. Commun. (1973) 158.
[18] E.R. Hamner, R.D.W. Kemmitt, M.A.R. Smith, J. Chem. Soc. Chem. Commun. (1974) 841.
[19] J. Burgess, R.I. Haines, R. Hamner, R.D.W. Kemmitt, M.A.R. Smith, J. Chem. Soc. Dalton Trans. (1975) 2579.
[20] G.K. Anderson, R.J. Cross, Acc. Chem. Res. 17 (1984) 67.
[21] K.J. Cavell, Coord. Chem. Rev. 155 (1996) 209.
[22] P.E. Garrou, R.F. Heck, J. Am. Chem. Soc. 98 (1976) 4115.
[23] S. Sakaki, K. Kitaura, K. Morokuma, K. Ohkubo, J. Am. Chem. Soc. 105 (1983) 2280.
[24] G.K. Anderson, R.J. Cross, J. Chem. Soc. Dalton Trans. (1980) 1434.
[25] S.A. Macgregor, Z. Lu, O. Eisenstein, R.H. Crabtree, Inorg. Chem. 33 (1994) 3616.
[26] B.A. Markies, P. Wijkens, A. Dedieu, J. Boersma, A.L. Spek, G. van Koten, Organometallics 14 (1995) 5628.
[27] R.H. Grubbs, A. Miyashita, M. Liu, P. Burk, J. Am. Chem. Soc. 100 (1978) 2418.
[28] G.K. Anderson, H.C. Clark, J.A. Davies, Inorg. Chem. 20 (1981) 3607.
[29] G.P.C.M. Dekker, C.J. Elsevier, K. Vrieze, P.W.N.M. van Leeuwen, Organometallics 11 (1992) 1598.
[30] G.K. Anderson, G.J. Lumetta, Organometallics 4 (1985) 1542.
[31] J.L. Hoare, K.J. Cavell, R. Hecker, B.W. Skelton, A.H. White, J. Chem. Soc. Dalton Trans. (1996) 2197.
[32] K. Frankcombe, K. Cavell, R. Knott, B. Yates, Chem. Commun. (1996) 781.
[33] K.E. Frankcombe, K.J. Cavell, B.F. Yates, R.B. Knott, Organometallics 16 (1997) 3199.
[34] H. Jin, K.J. Cavell, J. Chem. Soc. Dalton Trans. (1994) 415.
[35] S.Y. Desjardins, K.J. Cavell, H. Jin, B.W. Skelton, A.H. White, J. Organomet. Chem. 515 (1996) 233.
[36] S.Y. Desjardins, K.J. Cavell, J.L. Hoare, B.W. Skelton, A.N. Sobolev, A.H. White, W. Keim, J. Organomet. Chem. 544 (1997) 163.
[37] ADF 2.3.0, Theoretical Chemistry, Vrije Universiteit, Amsterdam, The Netherlands. (a) E.J. Baerends, D.E. Ellis, P. Ros, Chem. Phys. 2 (1973) 41. (b) C. Fonseca Guerra, O. Visser, J.G. Snijders, G. te Velde, in: E. Clementi, G. Corongiu (Eds.), Methods and Techniques for Computational Chemistry, STEFF, Cagliari, 1995, p. 305.
[38] G. te Velde, E.J. Baerends, J. Comp. Phys. 99 (1992) 84.
[39] (a) J.G. Snijders, E.J. Baerends, P. Vernooijs, At. Nucl. Data Tables 26 (1982) 483. (b) P. Vernooijs, J.G. Snijders, E.J. Baerends, Slater type basis functions for the whole periodic system, Internal Report, Free University of Amsterdam, The Netherlands, 1981.
[40] S.J. Vosko, L. Wilk, M. Nusair, Can. J. Phys. 58 (1980) 1200.
[41] L. Versluis, T. Ziegler, J. Chem. Phys. 88 (1988) 322.
[42] T. Ziegler, V. Tschinke, E.J. Baerends, J.G. Snijders, W. Ravenek, J. Phys. Chem. 93 (1989) 3050.
[43] A.D. Becke, Phys. Rev. A 38 (1988) 3098.
[44] J.P. Perdew, Phys. Rev. B 33 (1986) 8822.
[45] N. Koga, K. Morokuma, Chem. Rev. 91 (1991) 823.